# Delineation of contaminated aquifers using integrated geophysical methods in Northeast Punjab, Pakistan

Muhammad Hasan · Yanjun Shang ·
Gulraiz Akhter · Weijun Jin

**Abstract** A decline in surface water sources in Pakistan is continuously causing the over-extraction of groundwater resources which is in turn costing the saltwater intrusion in many areas of the country. The saltwater intrusion is a major problem in sustainable groundwater development. The application of electrical resistivity methods is one of the best known geophysical approaches in groundwater study. Considering the accuracy in extraction of freshwater resources, the use of resistivity methods is highly successful to delineate the fresh-saline aquifer boundary. An integrated geophysical study of VES and ERI methods was carried out through the analysis and interpretation of resistivity data using Schlumberger array. The main purpose of this investigation was to delineate the fresh/saline aquifer zones for exploitation and management of fresh water resources in the Upper Bari Doab, northeast Punjab, Pakistan. The results suggest that sudden drop in resistivity values caused by the solute salts indicates the saline aquifer, whereas high resistivity values above a specific range reveal the fresh water. However, the overlapping of fresh/saline aquifers caused by the formation resistivity was delineated through confident solutions of the D-Z parameters computed from the VES data. A four-layered unified model of the subsurface geologic formation was constrained by the calibration between formation resistivity and borehole lithologs. i.e., sand and gravel-sand containing fresh water, clay-sand with brackish water, and clay having saline water. The aquifer yield contained within the fresh/saline aquifers was measured by the hydraulic parameters. The fresh-saline interface demarcated by the resistivity methods was confirmed by the geochemical method and the local hydrogeological data. The proposed geophysical approach can delineate the fresh-saline boundary with 90% confidence in any homogeneous or heterogeneous aquifer system.

M. Hasan · Y. Shang · W. Jin
Key Laboratory of Shale Gas and Geoengineering, Institute of Geology and Geophysics, Chinese Academy of Sciences, Beijing 100029, China

Y. Shang
e-mail: jun94@mail.iggcas.ac.cn

W. Jin
e-mail: wjjin@mail.iggcas.ac.cn

M. Hasan · Y. Shang · W. Jin
Institutions of Earth Science, Chinese Academy of Sciences, Beijing 100029, China

M. Hasan · Y. Shang · W. Jin
University of Chinese Academy of Sciences, Beijing 100049, China

M. Hasan (✉)
Institute of Geology and Geophysics, Chinese Academy of Sciences, No. 19, Beitucheng Western Rd., Chaoyang District, Beijing 100029, P.R. China
e-mail: hasan.mjiinnww@gmail.com

G. Akhter
Department of Earth Sciences, Quaid-i-Azam University, Islamabad, Pakistan
e-mail: agulraiz@qau.edu.pk

## Introduction

Saltwater intrusion is the movement of salt water into the fresh aquifers (Hasan et al. 2018a). Salt-water inter-action is a type of groundwater pollution which gives rise to a protruding hydrological problem in many areas of the world (Post 2005). This phenomenon occurs due to the interruption in natural balance between the saline/ brackish and fresh aquifers mainly caused by human activity (Khwaja et al. 2001; Li et al. 2013). Saline intrusion is caused by certain factors such as excessive pumping of groundwater, low recharge rate, industrial waste materials, intensive farming, climate change, and natural events and so forth (Leghouchi et al. 2009; Barlow and Reichard 2010). The degree of saltwater intrusion differs from locality to locality based on the local hydrogeologic settings (Mondal et al. 2012; Kumar et al. 2016). Contamination by saline water may be of regional level and hence has significant consequence on groundwater supply (Mondal et al. 2011; Hasan et al. 2017a). In various cases, saline-water contamination is constrained only to small parts of the aquifer system and has no or less effects on the pumping wells (Capaccionia et al. 2005; Masoumi et al. 2019). Salt water intrusion arises where groundwater is being exploited from the fresh aquifer that is in hydrau-lic connection with the saline aquifer (Hasan et al. 2018b). Consequently, the induced gradient causes the saltwater to migrate from the saline aquifer towards the pumping well and so makes the freshwater well unfea-sible (Son 2011; Hasan et al. 2017b). Since the saltwater is denser than the freshwater, the freshwater floats over the saline aquifer, though the interface between the fresh and saline water is not distinct (Hasan et al. 2018a). Principally, groundwater flows from the areas with higher hydraulic head (groundwater level) towards those with lower hydraulic head (Simyrdanis et al. 2018). This natural movement of water causes the saline water intrusion. Saline water incursion has become one of the major challenges in hydrological studies as well as water management.

Groundwater is the main water supplier in many countries. In case of Pakistan, exploitation of ground-water resources especially for irrigated agriculture has rapidly increased over the last two decades (Rasool et al. 2015; Hasan et al. 2017a). Water supply from surface water sources such as rainfall, rivers, canals, and other water channels is continuously decreasing, whereas the demand for water supply is rapidly increasing. The main recharge of groundwater comes from the above sources. Insufficiency of surface water sources is causing over-withdraw of groundwater resources (Haq 2002). The Indus Basin of Pakistan holds one of the world's best irrigated canal systems with 31 million ha of the irrigat-ed land (MINFAL 2008). Currently, the World Bank conducted a survey suggesting that Pakistan has defi-cient of 50% water supply (Hasan et al. 2018a). Conse-quently, Pakistan is quickly becoming a water-scarce country (Qureshi et al. 2011; World Bank 2011). About 50% more tube-wells were installed during 2010–2017 in the Indus Basin of Pakistan (Pakistan Bureau of Statistics 2011; Hasan et al. 2018b). Out of the total 0.95 million tube-wells installed in Pakistan, the Upper Indus Basin in Punjab province alone holds about 0.79 million pumping-wells (Hasan et al. 2017a; Pakistan Bureau of Statistics 2011). Over-exploitation of the fresh water reserves through brisk installation of pumping boreholes lacking any geophysical or geotech-nical study has caused decline in water table as well as the saline water intrusion (Bakhsh and Awan 2002; Saeed 2008). Under such situations, an effective geo-physical investigation for the assessment of groundwa-ter resources including demarcation of the fresh-saline boundary and estimation of groundwater reserves is essential in order to exploit the fresh aquifers properly and maintain the water quality.

Generally, information about the groundwater quality is obtained by the traditional methods such as bore-wells through a number of laboratory analysis; however, such methods are quite expensive, intrusive, time taking, and cumbersome (Benabdelouahab et al. 2019). The use of geophysical methods is user-friendly, inexpensive, and non-invasive. Several investigations have used the 1D and 2D electrical resistivity methods for groundwater exploration (Hodlur et al. 2006; Bauer et al. 2006; Wilson et al. 2006; Soupios et al. 2007; Adepelumi et al. 2008; Kouzana et al. 2010; Baharuddin et al. 2011; Kura et al. 2014; Hasan et al. 2018c; Hasan et al. 2019a). Over the past decades, several studies were carried out to obtain the fresh-saline aquifer boundary only in the coastal areas (Cardona et al. 2004; Capaccionia et al. 2005; Barlow and Reichard 2010). However, most of the studies carried out in the alluvial plains do not clearly differentiate the fresh-saline inter-face where the overlapping of fresh-saline aquifers pre-vails. In this investigation, the electrical resistivity im-aging (ERI) coupled with the vertical electrical sound-ing (VES) were performed to mark out a boundary

between the saline/brackish and fresh aquifer for groundwater exploitation in the Upper Bari Doab of Punjab, Pakistan. In such methods, the subsurface resistivity of the geologic formation is obtained by inserting current through two current electrodes and computing potential by the potential electrodes using different configurations such as Schlumberger, Wenner, pole-pole, pole-dipole, and dipole-dipole. Resistivity differs from lithology to lithology (Mario et al. 2011). Resistivity of saline water is always less than that of fresh water (Hasan et al. 2019b). Similarly, clay formation shows low resistivity than that of sandy and gravel formation (Akhter and Hasan 2016; Hasan et al. 2017b). The electrical resistivity methods have advantage over other methods by measuring the formation resistivity in Ωm which has larger range than other units (Soupios et al. 2007). Different ERI profiles of about 1 km were conducted in the studied area which provides the fresh-saline aquifer interface with 2D imaging of subsurface layers. However, the fresh-saline water boundary over the entire area was delineated by the Dar-Zarrouk parameters specifically longitudinal conductance, longitudinal resistivity, and transverse resistance computed from ID geoelectrical method. Groundwater reserves associated with the saline and fresh water were measured using aquifer parameters such as transmissivity and hydraulic conductivity estimated from the VES method. The saline/brackish and fresh water zones delineated by the integrated geophysical method were confirmed by the physicochemical analysis.

This investigation was carried out to introduce an inexpensive and non-invasive geophysical approach to map an important boundary between the saline/brackish and fresh aquifers for proper utilization and management of the fresh aquifer reserves in the Upper Bari Doab of Punjab, Pakistan. The present research proposes cost-effectiveness of the integrated geophysical approach prior to installing the pumping boreholes.
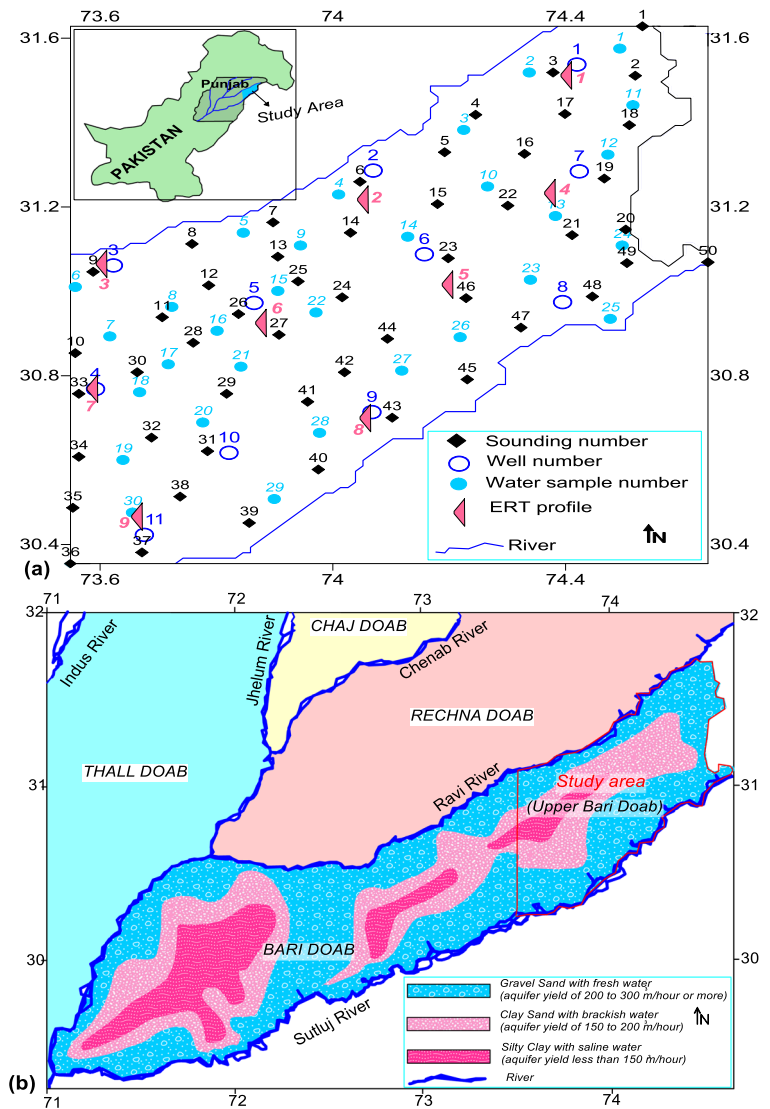
## Hydrogeological setting

The investigated area lies between the longitude 73.55°E and 74.64°E and the latitudes 30.35°N and 31.62°N in Punjab province of Pakistan as shown in Fig. 1a. The Upper Bari Doab has semiarid climate system. It has hot summer from April to September with mean and maximum temperature of 37 °C and 47 °C respectively. Its winter lasts from October to March with

mean and minimum temperature of 8 °C and 0 °C respectively. The mean annual rainfall in the Upper Bari Doab is about 305 mm with 457 mm in the northeast and 203 mm in the southeast. The Monsoon system is the main source of rainfall in the project area. About two-thirds of the annual rainfall comes during this season from June to September. The rest of precipitation falls during December and March, and although the winter rainfall is not sufficient, it is very important for the agriculture (WAPDA 1989). October and November are the driest months in the studied area. The Upper Bari Doab has a large alluvial plain shaped by Sutlej, Ravi and Bias River. It gently slopes between 179 and 215 m above mean sea level from northeast to southwest. The study area has relatively low runoff because of the gentle relief (WAPDA 1978).

The geological history of the Bari Doab is similar to that of the Chaj and Rechna Doabs. It has alluvial cover of Quaternary age that overlies the igneous and metamorphic rocks of Tertiary or Precambrian age. Basement rocks are entirely covered by the alluvial deposits. Precambrian rocks were revealed at different places during the special drilling in northeast of the project area. Red clays and gravels of fluviatile origin were found at a depth greater than 300 m during the deep drilling in the northeast which were marked different than the alluvial deposits. These units were named as unidentified units and interrelated with the Siwalik system. Alluvial cover is the main geological unit in which the groundwater reserves are contained. The dominant lithologies of the alluvial system revealed by the test drills include gravel-sand, clay-sand, sand and clay.

Generally, the alluvial cover has thickness of about 460 m with unconfined aquifer system (WAPDA 1978; IPD 2005). The brackish/saline aquifers with high salinity concentration are a challenging threat for agriculture and drinking purposes in the Upper Bari Doab (Hasan et al. 2017b). The transmissibility coefficients range from 0.2 to 1.0 cusecs per foot (WAPDA 1978). The permeability range is about 0.00033–0.01573 ft/s (WAPDA 1980). The lower storage coefficient is mainly because of the less permeable clay layers. The water level lies between 7 and 18 m. The aquifer system of the project area can be divided into three main units based on the local hydrogeological settings, i.e., high-yield aquifer, medium-yield aquifer, and low-yield aquifer. The high potential aquifer has fresh water through aquifer yield between 200 and 300 $m^3$/h containing gravel-sand and sand lithology. The medium-yield aquifer

Fig. 1 **a** Location map of the project area including geophysical, geochemical, and borehole measuring stations. **b** Map showing the simplified hydrogeological settings of the Bari Doab (modified after WAPDA 1989).



contains aquifer yield from 150 to 200 m³/h having brackish water and the main lithology such as clay-sand. The low-yield aquifer has aquifer potential less than 150 m³/h with clay. The simplified hydrogeological settings of the Bari Doab are shown in Fig. 1b (WAPDA 1989).

## Materials and methods

### VES and ERI methods

An integrated geophysical method involving 1D VES and 2D ERI was performed to obtain the formation resistivity for delineation of the saline/brackish and fresh water zones in the Upper Bari Doab. ERI was conducted along nine 2D profiles at different locations, whereas VES was carried out for 50 stations over the entire project area (Fig. 1a). The subsurface resistivity measurements were obtained by the ABEM Terrameter LS using the Schlumberger array with manual maximum electrode expansion of 200 m for VES and 150 m for ERI below the ground surface. The ABEM Terrameter LS was performed in such a way that the unreasonable resistivity values were neglected, and the measurements were repeated at the same spot to enhance the data quality. Resistivity acquired from the field measurements is known as the apparent resistivity given by

$$\rho_a = \frac{K\Delta V}{I} \tag{1}$$

The geometric factor K in the above equation is given by the relation:

$$K = \pi/2\left[(AB/2)^2 - (MN/2)^2\right]/(MN/2) \tag{2}$$

where $\rho$ is the apparent resistivity in $\Omega$m, AB is the electrode spacing, MN defines the distance between the potential electrodes, $I$ is current in Amp, and $V$ is the voltage in volts. The apparent resistivity values acquired from the field were drawn on a log–log graph against AB/2 (half-current electrode spacing). The basic principle to acquire the resistivity measurements is shown by a diagram in Fig. 2a.

A partial curve matching technique was used to obtain the qualitative and quantitative interpretation of VES curves. 1D inversion program of IPI2win software was performed for all 50 VES stations to generate a subsurface formation model having true resistivity and thickness of the subsurface geologic layers with least RMS error (< 5%).

ERI measurements along each profile were acquired within 40 min using electrode interval of 5 m, spread cable length of 840 m with 169 electrodes at 168 m take outs. Each electrode was checked through the electrode test to make sure the good ground-contact. Salt solution was used to enhance the performance of the electrodes having poor ground-contact.

The field data acquired by ERI survey was processed using the inversion program of RES2DINV (Loke et al. 2003). The software inverts 2D apparent resistivity into the pseudo-section of true resistivity using the least-squares technique (Gao et al. 2018; Loke and Barker 1996). The misfit between the measured and observed values of resistivity is minimized in the algorithm scheme. In this program, the subsurface formation is shown by a number of rectangular cells with constant resistivity values. At the beginning, a homogeneous resistivity value is assigned to each cell with a homogeneous resistivity value to generate an initial model; afterwards, the modeled resistivity is updated according to the misfit between the calculated and observed values in a pseudo-section after the iteration. The iterative process continues until a certain level of RMS error is obtained (Loke and Barker 1996; Hasan et al. 2018c). A smoothness constraint on the algorithm was used to acquire the interpreted ERI results. A pseudo-section

can be generated either by finite-element or finite-difference method. Since the study area has flat topography, finite-difference method was used in the present ERI investigation. A principle procedure to generate a pseudo section in ERI is shown in Fig. 2b.

D-Z and aquifer parameters

Sometimes, the results interpreted by the VES method show intermixing of resistivity values caused by the overlapping of the saline/brackish and fresh aquifers (Hasan et al. 2017b). As a result, the resolution is usually mired, and the uncertainty is prevailing. Dar-Zarrouk (D-Z) parameters estimated from the VES method can avoid overlapping caused by the saline/brackish and fresh water (Singh et al. 2004; Hasan et al. 2019b). The D-Z parameters such as longitudinal conductance, transverse resistance, and longitudinal resistivity are acquired through different arrangements of resistivity and thickness of the saturated geologic layers. The D-Z parameters are computed from the relations given by

$$S_c = h/\rho \tag{3}$$

$$T_r = h\rho \tag{4}$$

$$\rho L = h/S_c \tag{5}$$

where $S_c$ defines longitudinal unit conductance measured in units of mho or Siemens, $T_r$ is transverse unit resistance in $\Omega$m$^2$, and $\rho L$ is longitudinal resistivity in $\Omega$m. $\rho$ in $\Omega$m and $h$ in m are resistivity and thickness of the subsurface saturated layers respectively. Specific values range of D-Z parameters was obtained depending on the local hydrogeological information and the available boreholes data in the project area.

In order to estimate the yield of the fresh/saline aquifers, aquifer parameters including hydraulic conductivity and transmissivity were measured. First of all, transmissivity (Tp) and hydraulic conductivity (Kp) were determined at the selected eleven boreholes sites by the pumping test analysis using the Eden-Hazel technique with StepMaster (version 2.0) software. However, different empirical relations were obtained between the hydraulic and electrical parameters to estimate the fresh/saline aquifer yield over the entire area. First empirical relation was acquired between longitudinal
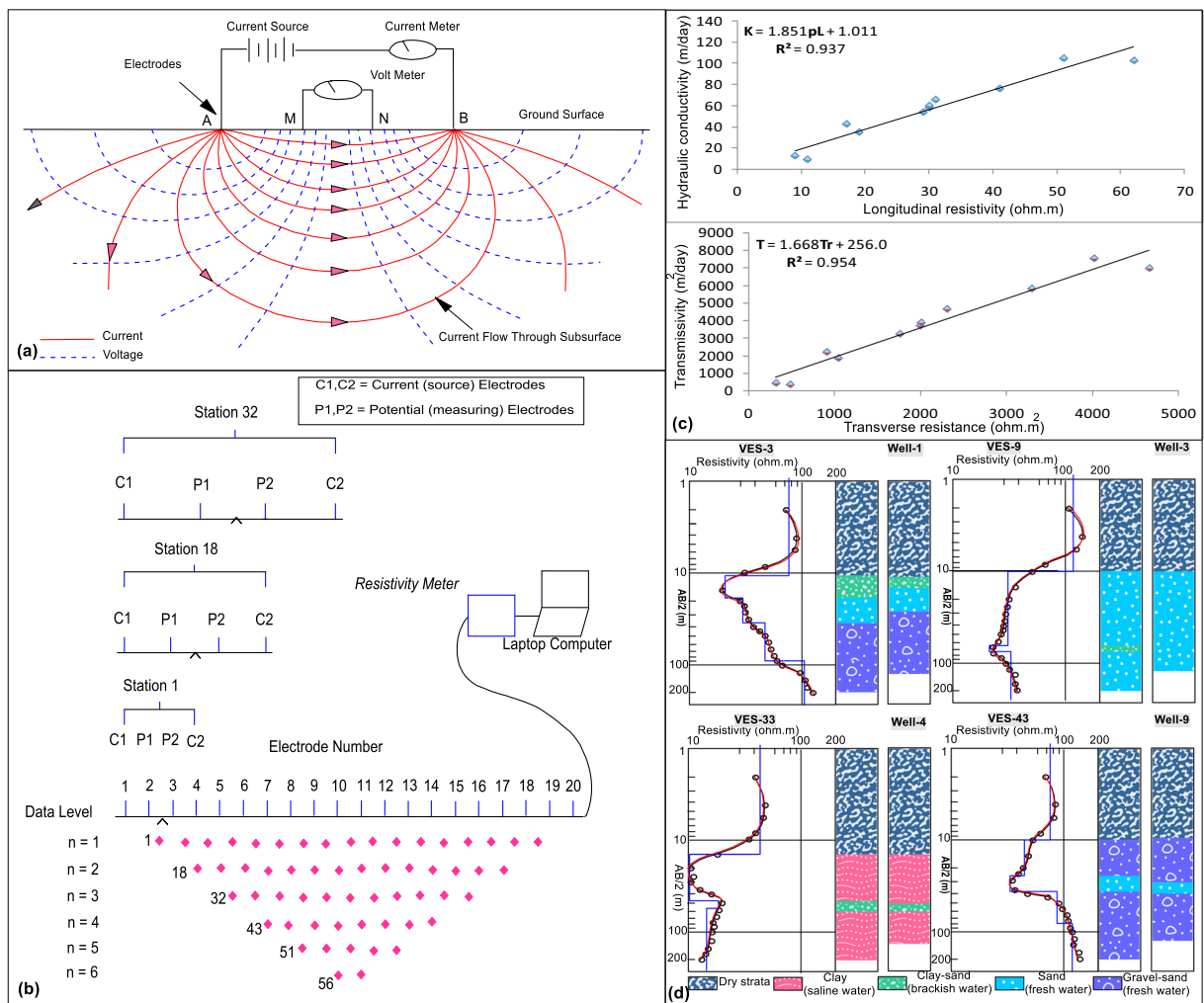
**Fig. 2 a** Fundamental conceptual model for resistivity measurement (modified after Todd and Mays 1980). **b** principle diagram to generate a pseudo section in ERI (adapted from ABEM Terrameter SAS4000/SAS1000 manual 2006). **c** Empirical relations between electrical parameters (longitudinal resistivity and transverse resistance) and measured hydraulic parameters (hydraulic conductivity and transmissivity). **d** Construction of VES geoelectrical columns and comparison with borehole lithologs for four stations

resistivity and pumped hydraulic conductivity (Fig. 2c), and another was established between transverse resistance and pumped transmissivity (Fig. 2c) given by

$$K = (1.851)*\rho L + 1.011 \tag{6}$$

$$T = (1.668)*T_r + 256 \tag{7}$$

where K is hydraulic conductivity in m/day and T is transmissivity in m$^2$/day.

Geochemical method

Total 30 groundwater samples collected at an average depth of 40–120 m from different places of the project area were analyzed by geochemical method for main anions including bicarbonates ($HCO_3^-$), chloride ($Cl^-$), nitrate ($NO_3^-$), and sulfates ($SO_4^{2-}$); main cations including potassium ($K^+$), magnesium ($Mg^{2+}$), sodium ($Na^+$), and calcium ($Ca^{2+}$); and other groundwater parameters for instance arsenic (As), electrical conductivity (EC), pH, and total dissolved solids (TDS) in the laboratory of Pakistan Council of Research in Water Resource (PCRWR) (Hasan et al. 2018a). The physicochemical analysis was carried out using ion chromatography method. Groundwater sampling was carried out through the filtration process using 0.45 μm membranes. After the filtration process, groundwater samples were put into two simulated polyethylene bottles.

Ionic concentration of the cations and anions was acquired using the standard procedures (Gao et al. 2018). EC with ± 1% and pH with ± 0.01 precision were measured by a multi-parameter analyzer (Hanna HI9829). Analysis of sulfates was performed using the UV–visible spectrophotometer. Bicarbonates were titrated on 100 ml of water using the volumetric technique with sulfuric acid as a titrand. The atomic absorption spectrometry and the volumetric method were used to analyze the main cations and anions respectively. Ionic concentration for all physicochemical parameters was acquired in milligrams per liter (mg/L) except pH, EC, and As. EC in microsiemens per centimeter (μS/cm) and As in ppb (parts per billion) were measured. The reliability of groundwater parameters was confirmed using the ionic balance of water between − 5% and + 5%.

## Results

### Construction of subsurface layered model

Apparent resistivity acquired in the field does not show true picture of the subsurface distinct layers (Hasan et al. 2018a). Therefore, the apparent resistivity obtained by VES and ERI is converted into true resistivity by the inversion program of software (Gao et al. 2018). The true resistivity is controlled by various factors including water and clay content, porosity, temperature, and fault etc. Resistivity of clay layer is lower than the sandy or gravel layer. Similarly, resistivity of saltwater is lower than that of freshwater. Generally, the saline water is associated with the clay formation and fresh water with the sandy formation (Hasan et al. 2018a). The modeled VES curves obtained by 1D inversion process of IPI2win software provides the information about the subsurface layers with thickness and resistivity of each layer.

However, limitations can be expected in the resistivity methods especially when there are anisotropy and homogeneity in the ground. Therefore, it is very important to restrain the subsurface geologic layers into a unified layered model through the calibration of VES results with the local boreholes data. In order to obtain non-predictive bias interpretation of the subsurface geologic formation, a calibration between the lithologs constructed from the boreholes data and the subsurface resistivity was performed. Rotary

including the DTH drilling rigs was used to acquire the lithologs from 11 bore-wells for calibration with the interpreted resistivity. Correlation between the VES resistivity and the borehole lithologs is given in Table 1. This correlation allowed delineating the subsurface geologic units with specific resistivity range of each layer and constructing the VES geoelectrical columns. The geoelectrical sections of the VES near the boreholes were constructed to map the depth and resistivity variations in the geologic formation. Four of such geoelectrical columns are given in Fig. 2d. The calibration between the borehole lithologs and the VES resistivity restrained the subsurface units into five discrete layers; for instance, the dry strata or topsoil cover (above water level), the clay layer having salt aquifer (below water level), the clay-sand geologic layer with brackish water (below water level), the sandy layer with fresh water (below water level), and the gravel-sandy layer having fresh water (below water level) through resistivity > 50 Ωm, < 15 Ωm, between 15 and 25 Ωm, from 25 to 40 Ωm, and > 40 Ωm respectively.

### Delineation of fresh-saline interface

Resistivity shows overlapping; therefore, it cannot delineate a discrete fresh-saline boundary. The D-Z parameters namely longitudinal conductance ($S_c$), traverse resistance ($T_r$), and longitudinal resistivity ($ρL$) computed from the VES method were used to obtain a distinct boundary between the saline, brackish, and fresh aquifer zones. These parameters were interpreted with specific value range based on the available borehole data and the local hydrogeological information. The fresh water

Table 1  Correlation between the boreholes data and the subsurface resistivity in the investigated area.

| Water table (water level) | Formation resistivity (in Ωm) | Type of lithology | Type of aquifer |
|---|---|---|---|
| Above water table | > 50 | Topsoil cover (dry strata) | – |
| Below water table | < 15 | Clay | Saline water |
| | 15–25 | Clay-sand | Brackish water |
| | 25–40 | Sand | Fresh water |
| | > 40 | Gravel-sand | Fresh water |

aquifer having sand and gravel-sand was revealed with $\rho L > 25$ $\Omega m$, $S_c < 2.6$ mho, and $T_r > 1400$ $\Omega m^2$. The saline water zone with clay was detected through $\rho L < 15$ $\Omega m$, $S_c > 3.3$ mho, and $T_r < 600$ $\Omega m^2$. The brackish water having clay-sand was marked by $\rho L$ between 15 and 25 $\Omega m$, $S_c$ from 2.6 to 3.3 mho, and $T_r$ between 600 and 1400 $\Omega m^2$. A clear interface with no overlapping between three distinct aquifers using $T_r$, $S_c$, and $\rho L$ is shown in Fig. 3a–c. The saline aquifer was revealed at five sounding stations, i.e., 25, 26, 28, 30, and 33; the brackish aquifer was delineated at 16 stations i.e., 10–16, 21–24, 27, 29, 32, and 34, whereas other stations indicate the fresh water as revealed in Fig. 3a–c. The VES interpretation reveals that the fresh water resources are found in the areas along rivers because the groundwater in these areas can be easily recharged by the river water. However, the areas with saline water are hardly recharged by the river water so such areas show high salinity level.

The hydraulic parameters namely hydraulic conductivity and transmissivity were determined to measure the potential of the fresh/saline aquifers delineated by the VES method. The aquifer potential of fresh water was estimated by K from 50 to 70 m/day for sand and > 70 m/day for gravel sand, T between 3000 and 5000 $m^2$/day for sand, and > 5000 $m^2$/day for gravel sand. The aquifer yield contained within the saline water was measured by K < 25 m/day and T < 1500 $m^2$/day containing clay. The brackish water which is intermixing zone between the saline and the fresh water was estimated with aquifer potential of K between 25 and 50 m/day and T between 1500 and 3000 $m^2$/day. The aquifer yield associated within the fresh, saline, and brackish water measured by hydraulic conductivity and transmissivity is shown in Fig. 3d, e. Good matching was found between the pumped and estimated hydraulic parameters for the selected stations as shown in Table 2.

ERI can delineate the fresh/saline aquifers both vertically and laterally along different profiles. The true resistivity of ERI was correlated with the nearby borehole lithologs to restrain a unified subsurface layered model to delineate the saline, brackish, and fresh aquifers. The fresh water zone containing sand and gravel-sand type lithologies was delineated by ERI resistivity > 25 $\Omega m$; the saline water containing clay was detected by resistivity < 15 $\Omega m$, and the brackish water having clay-sand was interpreted by resistivity from 15 to 25 $\Omega m$ (Fig. 4). Lithologs of bore-wells near the ERI profiles

were added to the interpreted pseudo-sections. The interpreted ERI results suggest that the fresh water aquifer is dominant alongside the rivers in profiles 1, 3, 8, and 9; the saline/brackish water aquifer is prevailing in profiles 4, 6, and 7, whereas profiles 2 and 5 show both fresh and saline/brackish aquifers. Being far away from the rivers and water channels, groundwater in profiles 4, 6, and 7 is not recharged enough so the salinity level is high. The interpreted fresh/saline aquifers in the ERI sections show strong correlation with the upfront boreholes. The ERI results suggest that the areas along profiles 1, 3, 8, and 9 are the most suitable places to exploit the fresh groundwater resources, whereas the rest of the areas are not appropriate for groundwater withdrawal.

Geochemical analysis

The saline, brackish, and fresh water zones revealed by ERI and D-Z parameters were confirmed by the geochemical analysis. The geochemical method was carried out for 30 groundwater samples collected from different sites in the project area. The suggested limits of WHO (WHO 2008) for groundwater parameters were used to perform the geochemical analysis. The physicochemical parameters which did not exceed the permissible limits of WHO were categorized as fresh water. On the other hand, those exceeding the suggested limits of WHO were interpreted into the saline or brackish aquifer. The geochemical interpretation reveals that almost all the physicochemical parameters exceeded the limits suggested by WHO for the saline aquifer, whereas some of the parameters exceeded the permissible limits for the brackish aquifer. The groundwater quality parameters were transformed into statistical study such as median, mean, maximum, minimum, and standard deviation as shown in Table 3. Figure 5 shows the groundwater samples with the saline, brackish, and fresh water interpreted by the geochemical method. The results suggest that the water samples 15–18 exceed the permissible limits for almost all physicochemical parameters and lie in the saline water zone, whereas samples 7–10, 13, 14, and 19–23 exceed the permissible limits for some of the physical parameters and lie in the brackish aquifer zone. The fresh, saline, and brackish aquifers interpreted through the geochemical method provide high correlation with those delineated by the integrated resistivity methods.
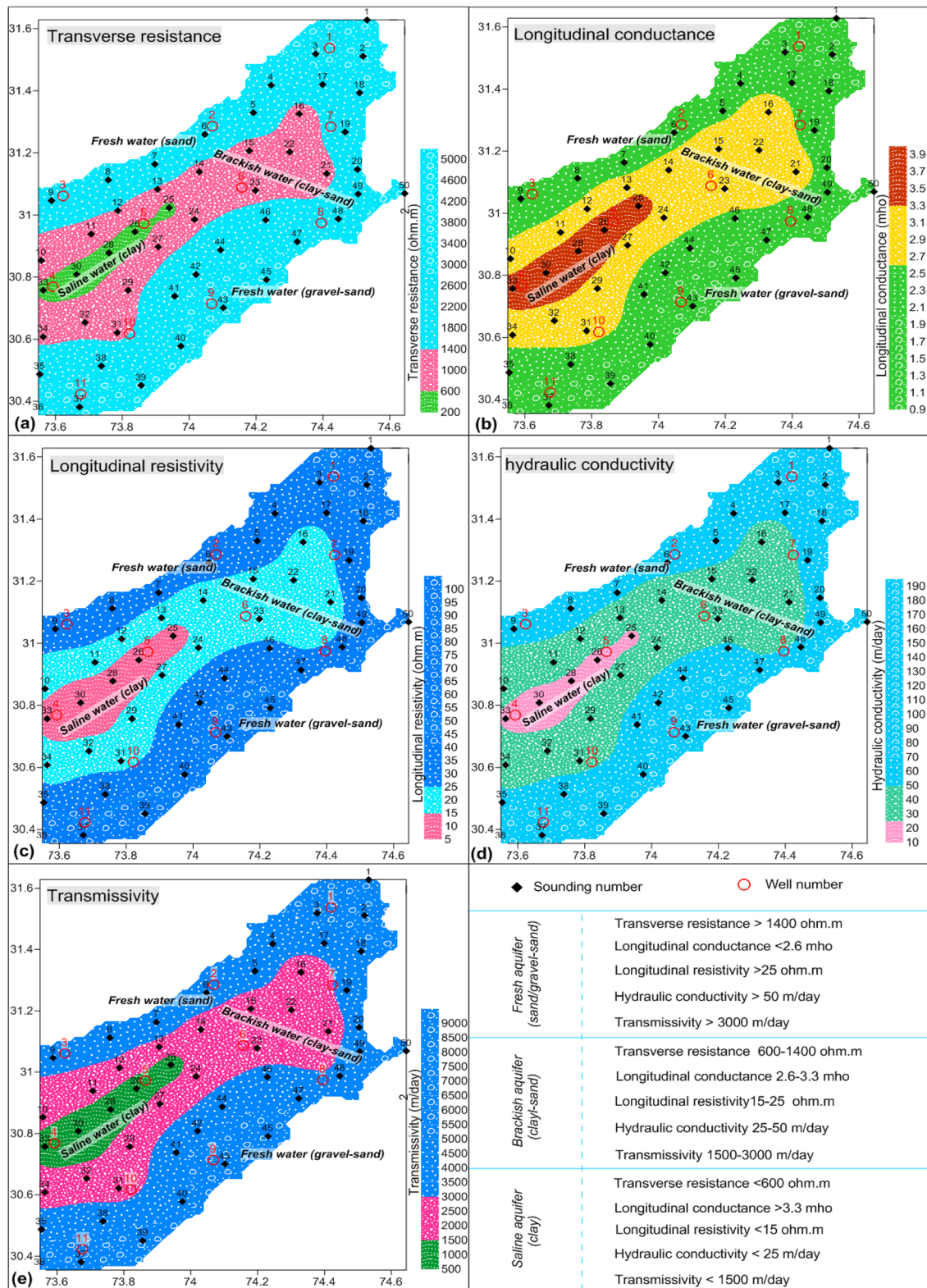
**Fig. 3** Delineation of saline, brackish and fresh water zones using **a** transverse resistance, **b** longitudinal conductance, **c** longitudinal resistivity, **d** hydraulic conductivity, and **e** transmissivity

**Table 2**  Comparison between the estimated and pumped aquifer parameters

| VES no. | Estimated parameters | | Well no. | Measured parameters | | % Matching | | %Error | |
|---|---|---|---|---|---|---|---|---|---|
| | Hydraulic conductivity K (m/day) | Transmissivity T (m²/day) | | Hydraulic conductivity $K_p$ (m/day) | Transmissivity $T_p$ (m²/day) | K and $K_p$ | T and $T_p$ | K and $K_p$ | T and $T_p$ |
| 3 | 77 | 5759 | 1 | 76 | 5852 | 99 | 98 | 1 | 2 |
| 6 | 58 | 4107 | 2 | 66 | 4686 | 88 | 87 | 12 | 13 |
| 9 | 57 | 3595 | 3 | 58 | 3712 | 98 | 97 | 2 | 3 |
| 33 | 21 | 1060 | 4 | 14 | 676 | 66 | 64 | 34 | 36 |
| 26 | 18 | 785 | 5 | 13 | 542 | 72 | 69 | 28 | 31 |
| 23 | 32 | 1784 | 6 | 43 | 2236 | 74 | 80 | 26 | 20 |
| 19 | 57 | 3605 | 7 | 60 | 3900 | 95 | 92 | 5 | 8 |
| 48 | 55 | 3198 | 8 | 54 | 3240 | 98 | 98 | 2 | 2 |
| 43 | 116 | 8034 | 9 | 103 | 7004 | 89 | 87 | 11 | 13 |
| 31 | 36 | 2001 | 10 | 35 | 1890 | 97 | 94 | 3 | 6 |
| 37 | 95 | 6961 | 11 | 105 | 7560 | 90 | 92 | 10 | 8 |

## Discussion

Saline intrusion is mainly caused by excessive pumping of groundwater, low recharge rate, industrial waste materials, intensive farming, climate change and natural events, and so forth. The intermixing of fresh water with the saline water is a threatening challenge in many countries. Therefore, the demarcation of fresh-saline water boundary is very essential to utilize and mange the groundwater resources. The present study was performed in the Upper Bari Doab of Punjab, Pakistan, to mark the boundary between the saline/brackish and fresh aquifers. However, demarcation of fresh-saline interface is not easy. Generally, the water quality is assessed by the traditional approaches such as the borehole methods. However, such techniques are expensive, time taking and intrusive, and still cannot delineate the saline/brackish and fresh water over a large area (Hasan et al. 2017b). The cost of a geophysical survey is directly related to how long it takes, the number and complexity of the instruments, and the size of the geophysical crew etc. Consequently, the cost ranges from less than US$1000 onwards. However, the cost ranges between US$2500 and 7500 for a geophysical survey that takes 1 to 3 days to complete. Generally, a borehole costs US$5500 for an average depth of 50 m. Mostly, the projects range between US$1500 and 1200. Applications of geophysical methods such as VES and ERI can efficiently mark out the boundary between the saline/brackish and fresh aquifers. Resistivity methods are cheap, user-friendly, and non-invasive and can evaluate the large area with confident results (Singh et al. 2004). However, the VES resistivity shows overlapping caused by the saline/brackish and fresh water. In order to obtain the confident solutions to delineate the saline/brackish and fresh aquifers, the D-Z parameters specifically transverse resistance, longitudinal resistivity, and longitudinal conductance were computed. The D-Z parameters delineated a clear boundary between the saline, brackish, and fresh aquifers over the entire investigated area. The ERI resistivity was estimated to demarcate the saline/brackish and fresh water zones in 2D pseudo-sections along the profiles. The fresh/saline aquifers revealed by D-Z parameters and ERI method show strong correlation. Furthermore, the subsurface formation was constrained by a model of four to five layers applicable to all VES stations and the ERI profiles. The model suggests that the topsoil cover consists of dry strata with formation resistivity above the water table, whereas the layers below water table were interpreted as clay layer with saline water, sandy clay having brackish water and gravel-sand and sand having fresh water. The saline/brackish and fresh aquifers interpreted by the geochemical method and the integrated geophysical methods show strong correlation. The aquifer yield of the fresh, saline, and brackish water was measured by the hydraulic parameters computed from the VES data. The results suggest that fresh water is found in the areas
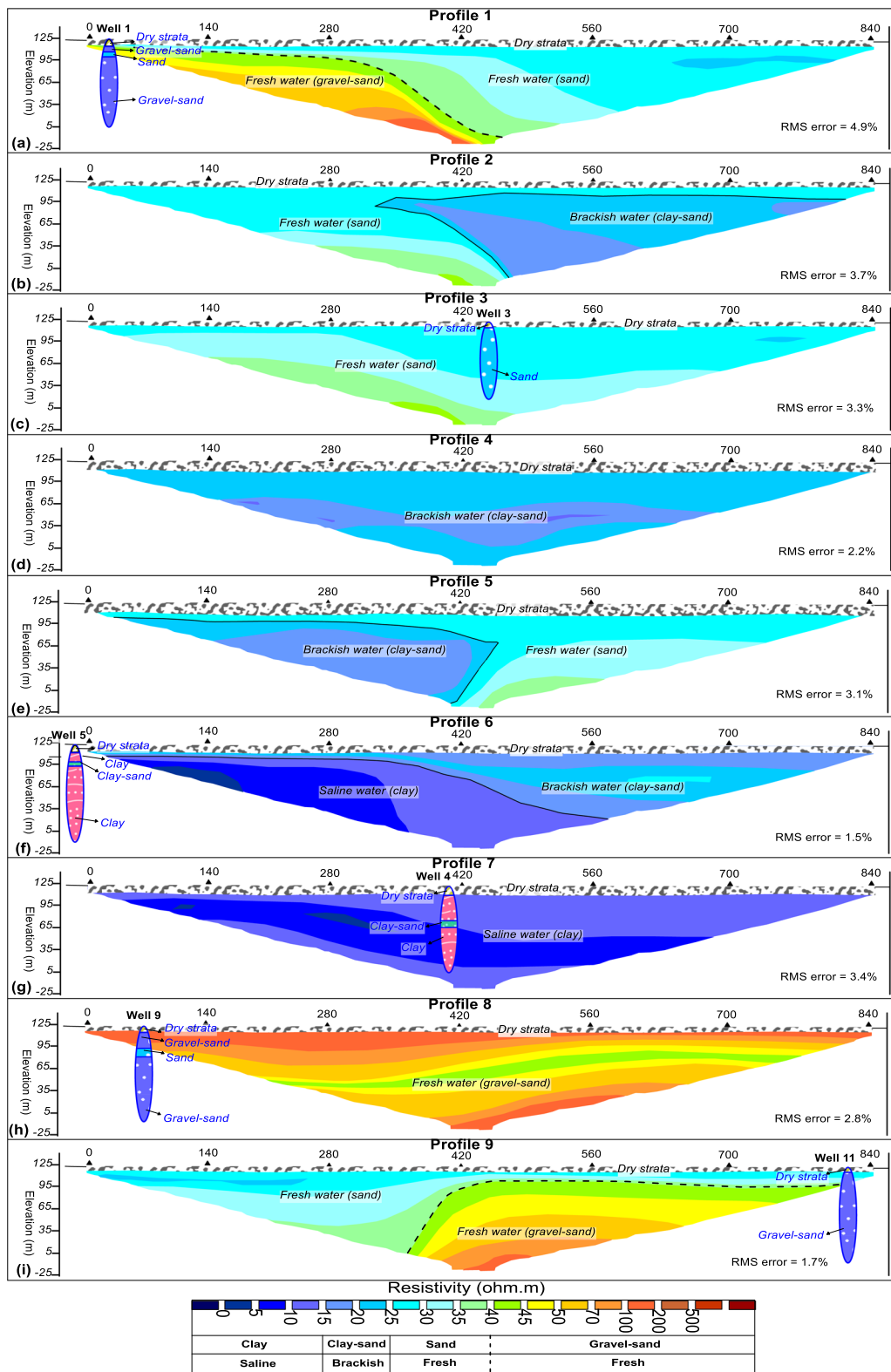
**Fig. 4** Demarcation of saline, brackish, and fresh aquifers using ERI along **a** profile 1, **b** profile 2, **c** profile 3, **d** profile 4, **e** profile 5, **f** profile 6, **g** profile 7, **h** profile 8, and **i** profile 9

**Table 3** The analysis of groundwater parameters statistically such as maximum, minimum, median, mean, and standard deviation, and the evaluation of groundwater quality using the recommended limits of WHO for the demarcation of saline, brackish, and fresh water

|  | Parameters | Units | Minimum | Maximum | Mean | Median | S.D. | WHO range | | |
|---|---|---|---|---|---|---|---|---|---|---|
|  |  |  |  |  |  |  |  | Fresh | Brackish | Saline |
| Cations | $Na^+$ | mg/L | 12 | 524 | 114 | 42 | 115.2 | < 150 | 150–200 | > 200 |
|  | $K^+$ | mg/L | 2 | 91 | 17.3 | 13 | 16.6 | < 30 | 30–55 | > 55 |
|  | $Ca^{2+}$ | mg/L | 10 | 272 | 93.4 | 82.2 | 61.2 | < 100 | 100–200 | >200 |
|  | $Mg^{2+}$ | mg/L | 10 | 121 | 48.3 | 46 | 24.2 | < 50 | 50–100 | > 100 |
| Anions | $Cl^-$ | mg/L | 18 | 642 | 163.4 | 191 | 129.8 | 200 | 200–250 | > 250 |
|  | $SO_4^{2-}$ | mg/L | 19 | 622 | 172.1 | 139 | 131.4 | < 150 | 150–200 | > 200 |
|  | $HCO_3^-$ | mg/L | 27 | 1136 | 428.2 | 448.3 | 237.2 | < 500 | 500–600 | > 600 |
|  | $NO_3^-$ | mg/L | 1 | 38 | 7.8 | 6 | 6.2 | < 7 | 7–10 | > 10 |
| Other parameters | EC | μS/cm | 242 | 6649 | 1515 | 959.4 | 1392.2 | < 750 | 750–1500 | > 1500 |
|  | TDS | mg/L | 161 | 4016 | 943.4 | 612 | 951.6 | < 500 | 500–1000 | > 1000 |
|  | As | ppb | 1 | 27 | 7.4 | 6.8 | 6.2 | 7 | 7–10 | > 10 |
|  | pH | – | 6.8 | 9.3 | 7.7 | 7.3 | 0.63 | < 7.5 | 7.5–8.5 | > 8.5 |

near rives, whereas the saline/brackish water is revealed in the central parts of the investigated area. The interpretations suggest that the proposed cost-effective geophysical approach can efficiently demarcate fresh/saline aquifers with over 80% assurance. The proposed resistivity approach can reduce important number of costly bore-wells and provide useful subsurface geologic information to demarcate the saline/brackish and fresh aquifers. The proposed geophysical approach can be effectively applied in homogenous as well as in heterogeneous aquifers with the integration of few boreholes. For monitoring of the fresh/saline aquifers, the time-lapse ERI survey is suggested to perform in order to predict the future migration of the fresh-saline water interface in the investigated area.

## Conclusion

An integrated geophysical approach involving 1D VES and 2D ERI was carried out in the alluvial plains of the Upper Bari Doab, Punjab, Pakistan. Purposed study was used to evaluate the subsurface layers particularly for the demarcation of the boundary between the saline/brackish and fresh water. The formation resistivity measured in the resistivity methods was correlated with the lithologs of the bore-wells to restrain a unified layered model appropriate to the entire study area. The unified layered

model restrained the subsurface units into five distinct layers for instance the topsoil cover, the clay layer, sandy clay layer, sandy layer, and the sandy gravel layer with specific aquifers and resistivity range such as dry strata having resistivity > 50 Ωm, saline aquifer containing resistivity < 15 Ωm, brackish water having resistivity from 15 to 25 Ωm, fresh aquifer with resistivity range of 25–40 Ωm, and fresh water containing resistivity > 40 Ωm, respectively. The D-Z parameters specifically transverse resistance ($T_r$), longitudinal conductance ($S_c$), and longitudinal resistivity ($ρL$) acquired by the VES data were used to mark a discrete boundary between the saline, brackish, and fresh aquifer. The fresh water was revealed with $T_r$ > 1400 Ωm$^2$, $ρL$ > 25 Ωm and $S_c$ < 2.6 mho. The brackish water was identified by $T_r$ between 600 and 1400 Ωm$^2$, $ρL$ between 15 and 25 Ωm, and $S_c$ range of 2.6–3.3 mho. The saline aquifer was delineated by $T_r$ < 600 Ωm$^2$, $ρL$ < 15 Ωm, and $S_c$ > 3.3 mho. The aquifer yield of the fresh, saline, and brackish water was measured by the hydraulic parameters including transmissivity (T) and hydraulic conductivity (K). The aquifer yield of the fresh water was estimated by T between 3000 and 5000 m$^2$/day for sand and > 5000 m$^2$/day for gravel sand, and K from 50 to 70 m/day for sand and > 70 m/day for gravel sand. The brackish water between the saline and fresh water was measured with aquifer yield of K from 25 to 50 m/day and T between 1500 and 3000
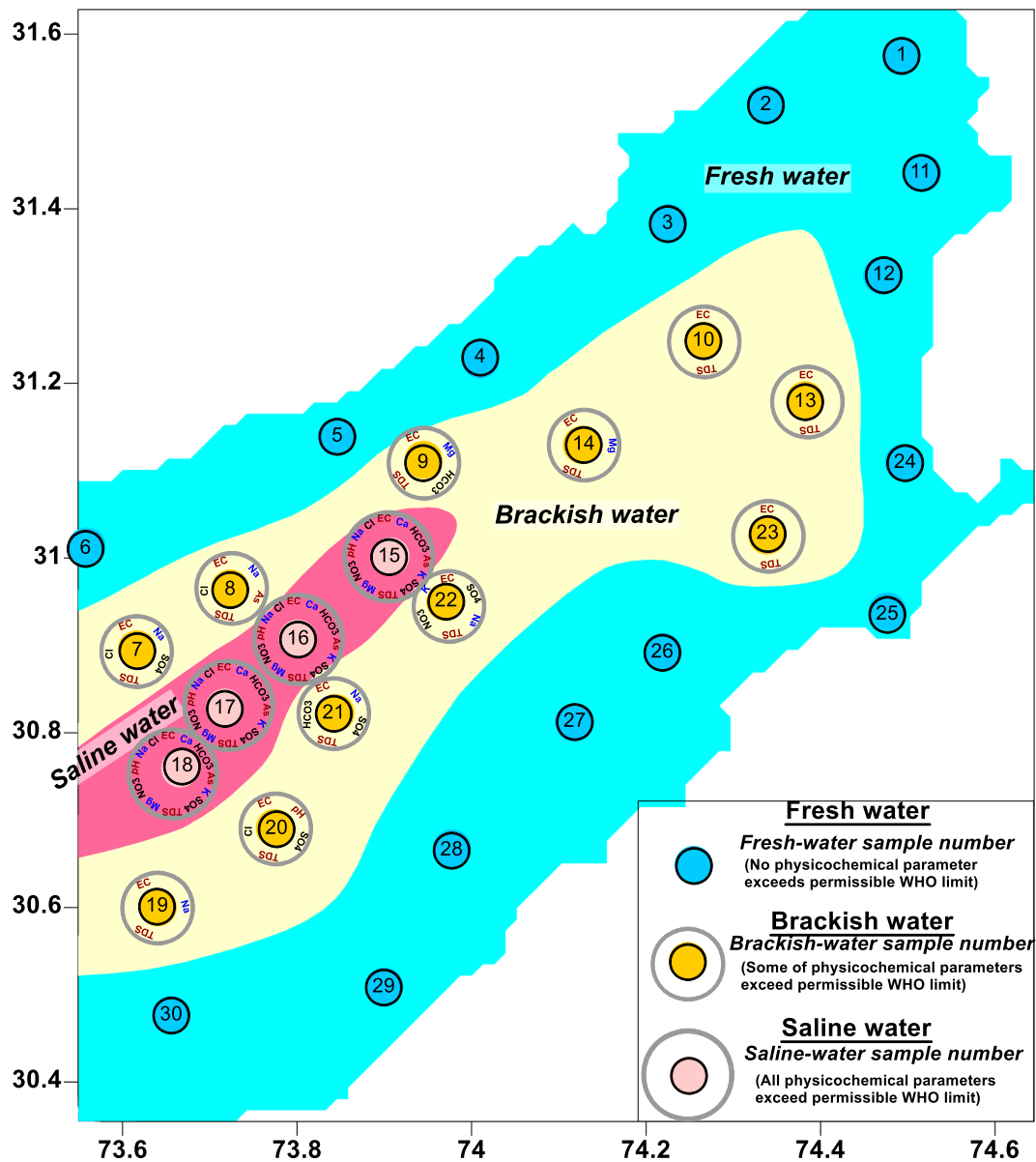
**Fig. 5** Demarcation of saline, brackish, and fresh water zones based on physicochemical analysis of geochemical method.

m²/day. The aquifer potential contained within the saline water zone was measured by K < 25 m/day and T < 1500 m²/day having clay. The saline, brackish, and fresh water zones revealed by ERI both vertically and horizontally along nine profiles show strong correlation with those demarcated by the D-Z parameters of VES method. The results of integrated geophysical approach for the differentiation of the boundary between the saline/brackish and fresh aquifer were confirmed by the geochemical method using the suggested limits of WHO. The results propose

that applications of integrated resistivity approach is economical and can reduce significant number of expensive bore-wells to acquire the subsurface information to delineate a boundary between the saline/brackish and fresh aquifer in any homogenous as wells as heterogeneous aquifer system.

Resources (PCRWR), Islamabad Pakistan, and Water and Power Development Authority (WAPDA), Pakistan.

**Compliance with ethical standards**

**Conflict of interest**  The authors declare that they have no conflict of interest.

# References

ABEM Instrument, AB. (2006). Terrameter SAS4000/SAS1000 LUND Imaging system, instruction manual.

Adepelumi, A. A., Ako, B. D., Ajayi, T. R., Afolabi, O., & Omotoso, E. J. (2008). Delineation of saltwater intrusion into the freshwater aquifer of Lekki Peninsula, Lagos, Niger. *Journal of Environmental Geology, 565*, 927–933.

Akhter, G., & Hasan, M. (2016). Determination of aquifer parameters using geoelectrical sounding and pumping test data in Khanewal District, Pakistan. *Open Geosciences, 8*, 630–638.

Baharuddin, M. F. T., Talib, S., Hashim, R., Abidin, M. H. Z., & Ishak, M. F. (2011). Time-lapse resistivity investigation of salinity changes at an ex-promontory land: a case study of Carey Island, Selangor, Malaysia. *Environmental Monitoring and Assessment, 180*, 345–369.

Bakhsh, A., & Awan, Q. A. (2002). Water issues in Pakistan and their remedies. In *National Symposium on Drought and Water Resources in Pakistan 16 March* (pp. 145–150). Lahore, Pakistan: CEWRE. University of Engineering and Technology.

Barlow, P. M., & Reichard, E. G. (2010). Saltwater intrusion in coastal regions of North America. *Hydrogeology Journal, 18*, 247–260.

Bauer, P., Supper, R., Zimmermann, S., & Kinzelbach, W. (2006). Geoelectrical imaging of groundwater salinization in the Okavango Delta, Botswana. *Journal of Applied Geophysics, 60*, 126–141.

Benabdelouahab, S., Salhi, A., Himi, M., Stitou el Messari, J. E., & Casas Ponsati, A. (2019). Geoelectrical investigations for aquifer characterization and geoenvironmental assessment in northern Morocco. *Environment and Earth Science, 78*, 209–216. https://doi.org/10.1007/s12665-019-8221-4.

Capaccionia, B., Diderob, M., Palettab, C., & Didero, L. (2005). Saline intrusion and re-freshening in a multilayer coastal aquifer in the Catania Plain (Sicily, Southern Italy): dynamics of degradation processes according to the hydrochemical characteristics of groundwater. *Journal of Hydrology, 307*, 1–16.

Cardona, A., Carrillo-Rivera, J. J., Huizar, A., Ivarez, R., & Graniel-Castro, E. (2004). Salinization in coastal aquifers of arid zones: an example from Santo Domingo, Baja California Sur, Mexico. *Environmental Geology, 45*, 350–366.

Gao, Q., Shang, Y., Hasan, M., Jin, W., & Yang, P. (2018). Evaluation of a weathered rock aquifer using ERT method in South Guangdong, China. *Water, 10*, 293.

Haq, A. U. (2002). Drought Mitigation interventions by improved water management: a case study from Punjab-Pakistan. In *In Proceedings of the 18th International Congress on Irrigation and Drainage, Montreal, Canada* (pp. 21–28) July.

Hasan, M., Shang, Y., Jin, W., & Akhter, G. (2019a). Investigation of fractured rock aquifer in South China using electrical resistivity tomography and self-potential methods. *Journal of Mountain Science, 16*(4), 850–869.

Hasan, M., Shang, Y., & Jin, W. (2018c). Delineation of weathered/fracture zones for aquifer potential using an integrated geophysical approach: a case study from South China. *Journal of Applied Geophysics, 157*, 47–60. https://doi.org/10.1016/j.jappgeo.2018.06.017.

Hasan, M., Shang, Y., Akhter, G., & Jin, W. (2017a). Geophysical assessment of groundwater potential: a case study from MianChannu area, Pakistan. *Groundwater, 56*, 783–796. https://doi.org/10.1111/gwat.12617.

Hasan, M., Shang, Y., Akhter, G., & Jin, W. (2018a). Delineation of saline-water intrusion using surface geoelectrical method in Jahanian area, Pakistan. *Water, 10*, 1548. https://doi.org/10.3390/w10111548.

Hasan, M., Shang, Y., Akhter, G., & Jin, W. (2018b). Evaluation of groundwater potential in Kabirwala area, Pakistan: a case study by using geophysical, geochemical and pump data. *Geophysical Prospecting, 66*, 1737–1750. https://doi.org/10.1111/1365-2478.12679.

Hasan, M., Shang, Y., Akhter, G., & Jin, W. (2019b). Application of VES and ERT for delineation of fresh-saline interface in alluvial aquifers of Lower Bari Doab. *Pakistan. Journal of Applied Geophysics., 164*, 200–213.

Hasan, M., Shang, Y., Akhter, G., & Khan, M. (2017b). Geophysical Investigation of fresh-saline water interface: a case study from South Punjab, Pakistan. *Groundwater, 55*, 841–856. https://doi.org/10.1111/gwat.12527.

Hodlur, G. K., Dhakate, R., & Andrade, R. (2006). Correlation of vertical electrical sounding and borehole-log data for delineation of saltwater and freshwater aquifers. *Geophysics, 7*, G11–G20.

Irrigation and Power Department (I&P). (2005). *A report on groundwater monitoring network of the directorate of land reclamation, Punjab*. Pakistan: Lahore.

Khwaja, A. R., Singh, R., & Tandon, S. N. (2001). Monitoring of Ganga water and sediments vis-a-vis tannery pollution at Kanpur (India): a case study. *Environmental Monitoring and Assessment, 68*(1), 19–35.

Kouzana, L., Benassi, R., Ben Mammou, A., & Felfoul, M. S. (2010). Geophysical and hydrochemical study of the seawater intrusion in Mediterranean semi arid zones. Case of the Korba coastal aquifer Cap-Bon, Tunisia. *Journal of African Earth Sciences, 582*, 242–254.

Kumar, V. S., Dhakate, R., Amarender, B., & Sankaran, S. (2016). Application of ERT and GPR for demarcating the saline water intrusion in coastal aquifers of Southern India. *Environment and Earth Science, 75*, 393.

Kura, N. U., Ramli, M. F., Ibrahim, S., Sulaiman, W. N., & Aris, A. Z. (2014). An integrated assessment of seawater intrusion in a small tropical island using geophysical, geochemical, and geostatistical techniques. *Environmental Science and*

*Pollution Research, 21*, 7047–7064. https://doi.org/10.1007/s11356-014-2598-0.

Leghouchi, E., Laib, E., & Guerbet, M. (2009). Evaluation of chromium contamination in water, sediment and vegetation caused by the tannery of Jijel (Algeria): a case study. *Environmental Monitoring and Assessment, 153*(1-4), 111–117.

Li, P., Wu, J., & Qian, H. (2013). Assessment of groundwater quality for irrigation purposes and identification of hydrogeochemical evolution mechanisms in Pengyang County. *China Environ Earth Sci, 69*, 2211–2225. https://doi.org/10.1007/s12665-012-2049-5.

Loke, M. H., & Barker, R. D. (1996). Rapid least-squares inversion of apparent resistivity pseudosections by a quasi-Newton method. *Geophysical Prospecting, 44*, 131–152.

Loke, M. H., Acworth, I., & Dahlin, T. (2003). A comparison of smooth and blocky inversion method in 2D electrical tomography surveys. *Exploration Geophysics, 34*, 182–187.

Mario, Z., Joan, B., Rogelio, L., & Xavier, M. P. (2011). Electrical methods (VES and ERT) for identifying, mapping and monitoring different salinedomains in a coastal plain region (Alt Emporda, Northern Spain). *Journal of Hydrology, 409*, 407–422.

Masoumi, M., Mahmudy Gharaie, M. H., & Ahmadzadeh, H. (2019). Assessment of groundwater quality for the irrigation of melon farms: a comparison between two arable plains in northeastern Iran. *Environment and Earth Science, 78*, 214–217. https://doi.org/10.1007/s12665-019-8187-2.

Ministry of Food Agriculture and Livestock (MINFAL). (2008). *Agricultural statistics of Pakistan*. Islamabad, Pakistan: Government of Pakistan (Economic Wing).

Mondal, N. C., & Singh, V. P. (2012). Chloride migration in groundwater for a tannery belt in Southern India. *Environmental Monitoring and Assessment, 184*(5), 2857–2879.

Mondal, N. C., Singh, V. P., Singh, S., & Singh, V. S. (2011). Hydrochemical characteristic of coastal aquifer from Tuticorin, Tamil Nadu, India. *Environmental Monitoring and Assessment, 175*(1-4), 531–550.

Pakistan Bureau of Statistics. (2011). Agricultural statistics of Pakistan 2010-11. In *Statistics Division Government of Pakistan*. Islamabad: Statics House, 21-Mauve area, G-9/1.

Post, V. E. A. (2005). Fresh and saline groundwater interaction in coastal aquifers: Is our technology ready for the problems ahead. *Hydrogeology Journal, 13*, 120–123.

Qureshi, A. L., Lashari, B. K., Kori, S. M., & Lashari, G. A. (2011). Hydro-salinity behaviour of shallow groundwater. In *Paper presented at the Fifteenth International Water Technology Conference, IWTC-15*. Alexandria: Egypt.

Rasool, A., Xiao, T., Baig, Z. T., Masood, S., Mostofa, K. M. G., & Iqbal, M. (2015). Co-occurrence of arsenic and fluoride in the groundwater of Punjab, Pakistan: source discrimination and health risk assessment. *Environmental Science and Pollution Research, 23*(13), 13578–13580.

Saeed, M. M. (2008). *Skimming Wells*. Islamabad, Pakistan: Higher education commission.

Simyrdanis, K., Papadopoulos, N., Soupios, P., Kirkou, S., & Tsourlos, P. (2018). Characterization and monitoring of sub-surface contamination from Olive Oil Mills' waste waters using electrical resistivity tomography. *Science of the Total Environment, 637-638*, 991–1003. https://doi.org/10.1016/j.scitotenv.2018.04.348.

Singh, U. K., Das, R. K., & Hodlur, G. K. (2004). Significance of Dar-Zarrouk parameters in the exploration of quality affected coastal aquifer systems. *Environmental Geology, 455*, 696–702.

Son, Y. (2011). Assessment of concentration in contaminated soil by potentially toxic elements using electrical properties. *Environmental Monitoring and Assessment, 176*, 1–11.

Soupios, P. M., Kouli, M., Vallianatos, F., Vafidis, A., & Stavroulakis, G. (2007). Estimation of aquifer hydraulic parameters from surficial geophysical methods: a case study of Keritis Basin in Chania (Crete–Greece). *Journal of Hydrology, 338*, 122–131.

Todd, D. K., & Mays, L. W. (1980). *Groundwater hydrology* (3rd ed.). Hoboken, NJ: John Wiley & Sons.

Water and Power Development Authority (Pakistan). (1978). Hydro geological data of Lower Bari Doab. *V, 01*.

Water and Power Development Authority (Pakistan). (1980). Hydro geological data of Lower Bari Doab. *V, 01*, 1.

Water and Power Development Authority (WAPDA). (1989). Annual reports 1988-89. *Lahore*, 21–98.

Wilson, S. R., Ingham, M., & Mcconchie, J. A. (2006). The ability of earth resistivity methods for saline interface definition. *Journal of Hydrology, 316*, 301–312.

World Bank. (2011). Annual report 2011, year in review. In *1818 Washington DC* (p. 20433). isbn:9780821388280.

World Health Organization (WHO). (2008). Guidelines for drinking-water quality. In *Recommendations Incorporating1ST and 2nd Addenda* (Vol. Volume 1, 3rd ed.). Geneva, Switzerland: World Health Organization.